The Same IκBα Mutation in Two Related Individuals Leads to Completely Different Clinical Syndromes

Riny Janssen,[1] Annelies van Wengen,[1] Marieke A. Hoeve,[2] Monique ten Dam,[3] Miriam van der Burg,[4] Jacques van Dongen,[4] Esther van de Vosse,[1] Maarten van Tol,[3] Robbert Bredius,[3] Tom H. Ottenhoff,[2] Corry Weemaes,[5] Jaap T. van Dissel,[1] and Arjan Lankester[3]

[1]*Department of Infectious Diseases,* [2]*Department of Immunohematology and Bloodtransfusion, and* [3]*Department of Pediatrics, Leiden University Medical Center, 2300 RC Leiden, Netherlands*
[4]*Department of Immunology, Erasmus Medical Center, Erasmus University, 3015 GE Rotterdam, Netherlands*
[5]*Department of Pediatrics, University Medical Center, 6500 HB Nijmegen, Netherlands*

The Journal of Experimental Medicine

Downloaded from http://rupress.org/jem/article-pdf/200/5/559/1151690/jem2005559.pdf by guest on 29 May 2022

Abstract

Both innate and adaptive immune responses are dependent on activation of nuclear factor κB (NF-κB), induced upon binding of pathogen-associated molecular patterns to Toll-like receptors (TLRs). In murine models, defects in NF-κB pathway are often lethal and viable knockout mice have severe immune defects. Similarly, defects in the human NF-κB pathway described to date lead to severe clinical disease. Here, we describe a patient with a hyper immunoglobulin M–like immunodeficiency syndrome and ectodermal dysplasia. Monocytes did not produce interleukin 12p40 upon stimulation with various TLR stimuli and nuclear translocation of NF-κB was impaired. T cell receptor–mediated proliferation was also impaired. A heterozygous mutation was found at serine 32 in IκBα. Interestingly, his father has the same mutation but displays complex mosaicism. He does not display features of ectodermal dysplasia and did not suffer from serious infections with the exception of a relapsing *Salmonella typhimurium* infection. His monocyte function was impaired, whereas T cell function was relatively normal. Consistent with this, his T cells almost exclusively displayed the wild-type allele, whereas both alleles were present in his monocytes. We propose that the T and B cell compartment of the mosaic father arose as a result of selection of wild-type cells and that this underlies the widely different clinical phenotype.

Key words: immunodeficiency • IκBα • monocyte function • T cell activation • infection

Introduction

Recognition of pathogen-associated molecular patterns (PAMPs) via Toll-like receptors (TLRs) is a crucial step in the human defense. Both innate and adaptive immune responses are thought to be highly dependent on signal transduction induced upon ligation of such receptors, and it is now well established that mice that lack specific TLRs, or components necessary for TLR-mediated signal transduction, are highly susceptible to specific pathogens. For instance, mice deficient for TLR4, which is important for recognition of LPS, a component of the cell wall of Gram-negative bacteria, are very susceptible to infection by *Salmonella* (1), whereas susceptibility to *Mycobacterium avium* (2) or *Toxoplasma gondii* (3) infection is not affected. Mice deficient for TLR2, which is important for the recognition of cell wall components of Gram-positive bacteria, are susceptible to infection with *Staphylococcus aureus* (4) or *M. avium* (2). On the other hand, MyD88-defective mice, which lack a common signaling protein involved in signal transduction via several TLRs, are highly susceptible to virtually every pathogen tested (2, 4–6), indicating the importance of recognition of PAMPs in combating a wide range of infections.

Upon ligation of TLRs, signal transduction is initiated, resulting in the activation of MAP kinases and NF-κB (for review see reference 7), the latter one being responsible for

J.T. van Dissel and A. Lankester contributed equally to this work.

Address correspondence to Riny Janssen, Dept. of Infectious Diseases, C5-P Leiden University Medical Center, P.O. Box 9600, 2300 RC Leiden, Netherlands. Phone: 31-71-526-2204; Fax: 31-71-626-6758; email: C.M.Janssen@lumc.nl

Abbreviations used in this paper: IKK, IκB kinase; JIA, juvenile idiopathic arthritis; PAMP, pathogen-associated molecular pattern; TLR, Toll-like receptor; TT, tetanus toxoid.

J. Exp. Med. © The Rockefeller University Press • 0022-1007/2004/09/559/10 $8.00
Volume 200, Number 5, September 6, 2004 559–568
http://www.jem.org/cgi/doi/10.1084/jem.20040773

the induction of proinflammatory cytokine production. In resting cells, the inhibitor of NF-κB, IκB, associates with NF-κB, thereby inhibiting its nuclear translocation and the transcription of NF-κB–responsive genes. In response to TLR ligation, IκB is phosphorylated through the action of the IκB kinase (IKK) complex (consisting of IKKα, IKKβ, and NEMO) and subsequently ubiquitinated and degraded by the proteasome, allowing translocation of NF-κB to the nucleus (for review see reference 8). Patients with various defects in PAMP-induced signal transduction have been described. For instance, patients with defects in NEMO, the regulatory subunit of the IKK complex that phosphorylates IκB, suffer from a broad clinical spectrum of disease including ectodermal dysplasia, high IgM, and susceptibility to a broad range of infectious agents (9). Recently, defects in IRAK4, one of the proteins upstream of IKK-dependent IκB phosphorylation, have been reported (10, 11). The four patients described to date suffered from pyogenic infections.

In murine models, defects in the NF-κB signaling pathway are often lethal, and knockout mice that are viable have severe defects in immune cell function, highlighting the importance of this signal transduction pathway in mice (for review see references 8 and 12). Similarly, defects in the human NF-κB pathway that have been described to date all lead to a relatively severe clinical syndrome (10, 11, 13), suggesting that optimal signal transduction via this pathway is also crucial in humans. However, because case finding is biased toward the identification of patients with severe symptoms, the true importance of this signal transduction pathway in the development of human disease is not known. Here, we describe a patient with a hyper IgM-like immunodeficiency syndrome with ectodermal dysplasia. Both T cell and monocyte function were severely impaired in this patient, and we found the mutation responsible for this syndrome in the IκBα gene. Interestingly, his father, who has the same mutation, does not display ectodermal dysplasia nor severe infection susceptibility. These cases illustrate that genetic mutations in components of the NF-κB signaling pathway do not necessarily lead to a life-threatening clinical phenotype.

Materials and Methods

Case Reports. A male infant was born as the first child to nonconsanguineous Caucasian parents after an uncomplicated pregnancy of 39^{+3} wk. At birth, his weight and length were 3,175 g (SD −1) and 49 cm (SD −1), respectively. Physical examination at birth revealed no abnormalities. Other than mild cutaneous candidiasis, there were no major complications during the first 2 mo of life. At the age of 2 mo, he presented with clinical signs of meningitis. β-hemolytic group A streptococcus was cultured from the cerebrospinal fluid. He made a rapid and complete recovery after treatment with parenteral antibiotics. However, a persistent leukocytosis was present during follow-up (20–35 × 10e9/L) with a polyclonal lymphocytosis of 55–80%. At the age of 4 mo, he presented with fever and dyspnea. Chest X ray revealed an interstitial infiltrate compatible with a diagnosis of pneumonia. A β-hemolytic group A streptococcus was isolated again from blood cultures. This time, clinical improvement was only moderate after antibiotic treatment, and he remained tachypneic and required continuation of oxygen. In bronchoalveolar lavage fluid, *Pneumocystis carinii* was identified. The patient recovered rapidly during treatment with high dose cotrimoxazole. Subsequent immunological evaluation revealed an agammaglobulinemia (0.5 g/L; see Table I) with a strongly increased serum IgM. Again, leukocytosis persisted after recovery from the infection. The lymphocytosis predominated with a CD4/CD8 ratio of 2.1–2.8:1 and was almost exclusively composed of naive ($CD45RA^+$) T lymphocytes. Hyper IgM syndrome was considered, but CD154 was expressed normally on activated T lymphocytes. Sequence analysis of the CD154, CD40, AID, and NEMO genes revealed no mutations (not depicted). Sequencing analysis of IGG and IGA transcripts showed that somatic hypermutations were present, although in low frequencies (∼2%; not depicted). Immunological findings of the patient and his parents are summarized in Table I. Based on chromosomal studies, we could exclude ataxia telangiectasia, Nijmegen breakage syndrome, and ICF syndrome (not depicted). From the second infection onwards, Ig substitution was initiated together with cotrimoxazole as *P. carinii* prophylaxis. Except for intermittently recurrent mucosal candidiasis that responded to fluconazole, no subsequent serious infections were encountered during follow-up. At the age of 2 yr, the patient was vaccinated with tetanus toxoid (TT) and diphtheria toxoid, inactivated poliovirus, and *Haemophilus influenzae* conjugate, and was boosted twice. No seroconversion was documented for all of the antigens tested (not depicted). After the first months of life, several signs of ectodermal dysplasia became manifest and comprised abnormal dentition (typical conical teeth) and periorbital wrinkling. During the first 2 yr of life, a retardation in neuromotor development became obvious, characterized by a delay in speech development and the inability to walk. A growth retardation became evident after the first 6 mo, starting at −1 SD and declining below −2 SD at the age of two. The latter two phenomena are not common features of ectodermal dysplasia syndromes. In addition, he developed periodic diarrhea and oral feeding was less well tolerated. Stool analysis for bacterial, viral, and parasitic infections by culture and microscopy remained negative. During his second year he became dependent on nasogastric hyper-alimenation. At the age of 2.5 yr, the boy was scheduled for allogeneic stem cell transplantation, which will be described separately.

The patients' father was born from nonconsanguineous Caucasian parents. At the age of two, he presented with arthritis of the knee that resolved spontaneously. After a disease-free interval of 6 yr, he developed fever, a typical rash, and arthritis. Systemic juvenile idiopathic arthritis (JIA) was diagnosed and steroid treatment was initiated and continued until the age of 17. After a therapy-free interval of ∼2 yr, he developed a *Salmonella typhimurium* enteritis that was treated with chloramphenicol. During the next 1.5 yr, the *S. typhimurium* infection persisted with recurrent manifestations in psoas muscle, pleural cavity, pericardial fluid, and ribs. 10 yr ago, two ribs and preural schwarte were resected. The infection finally resolved after prolonged treatment with cotrimoxazole and amoxicillin. After a 7-yr, symptom-free interval, he developed rheumatoid factor–positive oligoarthritis, which resolved upon treatment with nonsteroid antiinflammatory drugs. Presently, he has no health complaints and is not taking any medication. Serum Ig levels and lymphocyte counts are within the normal range and a normal ratio between naive and memory T lymphocytes is present (see Table I).

Isolation of PBMCs and Culture of Human Monocyte–derived Macrophages. PBMCs were isolated from heparinized blood using density centrifugation over a Ficoll-Hypaque gradient (Amer-

Downloaded from http://rupress.org/jem/article-pdf/200/5/559/1151690/jem2005559.pdf by guest on 29 May 2022

sham Biosciences). For generation of macrophages, PBMCs were cultured in 6-well tissue culture plates (Costar) in Dulbecco's modified Eagle's medium (GIBCO BRL) supplemented with 2 mM L-glutamine, 100 U/ml penicillin, 0.1 mg/ml streptomycin, and 10% heat-inactivated pooled human serum. After 24 h, nonadherent cells were removed by extensive washing and cells were cultured for 6 d to obtain monocyte-derived macrophages. Cells were trypsinized and adhered onto glass coverslips, and then cultured for another 2–3 d. Any remaining nonadherent cells were washed away, and relatively pure (>95%) monocyte-derived macrophage populations were obtained.

Lymphocyte Proliferation. Triplicate cultures of 0.4×10^5 PBMCs or 0.2×10^5 $CD20^+$ B cells per well in medium (RPMI 1640 glutamax 1 [GIBCO BRL] supplemented with 10% heat-inactivated pooled human AB serum, 100 U/ml penicillin [GIBCO BRL], and 100 μg/ml streptomycin [GIBCO BRL]) were performed in 96-well, flat-bottom microtitre plates (Costar) using 5 μg/ml PHA (Murex), 50 IU/ml IL-2 (Chiron Corp.), 500 ng/ml anti-CD40 (Beckman Coulter), 500 U/ml IL-4 (PeproTech), and coated anti-CD3 (0.1 μg/ml OKT3 in PBS; Ortho Clinical Diagnostics) as stimuli.

After 4 d of culture, 1 μCi/well [^{3}H]thymidine (Amersham Biosciences) was added 18 h before harvesting. [^{3}H]thymidine uptake of cultured PBMCs was measured as cpm by liquid scintillation counter (Wallac). Triplicate cultures of 10^5 PBMCs per well were performed in 96-well, round-bottom microtitre plates (Costar) in medium. Cells were cultured for 5 d with 2 LF/ml TT (RIVM) followed by the addition of [^{3}H]thymidine as described above. Results are shown as a stimulation index (ratio mean cpm TT/mean cpm medium). A stimulation index of ≥3.0 was considered evidence of antigen-induced proliferation.

Immunophenotyping and Sorting of Lymphocytes. PBMCs were phenotyped by four color immunostaining using FITC-, PE-, PerCPCy5.5-, and APC-conjugated antibodies, and analyzed by flow cytometry (FACSCalibur; Becton Dickinson). Data were analyzed using CELLQuest software (Becton Dickinson). Cell sorting was performed on a FACS Vantage (Becton Dickinson).

Stimulation of Whole Blood. Blood collected in endotoxin-free tubes (Endotube ET; Chromogenix) was diluted 1 in 5 and stimulated overnight with 0.1–1,000 ng/ml LPS in the presence or absence of 10–1,000 IU IFN-γ/ml. Other TLR stimuli used were 25 μg/ml *M. avium* sonicate, 100 μg/ml zymosan A, *S. aureus* (5×10^6 heat-killed bacteria/ml), and 200 ng/ml PAM3CSK4. Supernatants were tested by ELISA for the presence of IL-12p40 (R&D Systems), IL-6, IL-1β, and TNF-α (Sanquin Research).

IFN-γ Responsiveness of Monocytes. PBMCs were incubated overnight with increasing amounts of IFN-γ (0–100 IU/ml) in hydron-coated wells to prevent adherence of the monocytes. Cells were washed and stained with FITC-conjugated anti-CD64 and PE-conjugated anti-CD14 to analyze CD64 expression on $CD14^+$ cells using a FACSCalibur.

Oxidative Burst. PMNs were isolated from whole blood by centrifugation over a Ficoll-Hypaque gradient (Amersham Biosciences). Red blood cells in the pellets were lysed using 180 mM NH4Cl for 20 min. Neutrophils were incubated with 5 μg/ml LPS or 200 ng/ml TNF-α for 30 min. After the addition of 10 μM DCF-DA, cells were incubated with 1 μM formyl-methionyl-leucyl-phenylalanine for 5 min and fluorescence was measured by FACS analysis.

NF-κB Translocation to the Nucleus. Monocyte-derived macrophages cultured on glass coverslips were incubated with 1,000 ng/ml LPS or 200 ng/ml TNF-α for 45 min, and p65 translocation to the nucleus was analyzed (14). Cells were fixed with paraformaldehyde and permeabilized with methanol. Cells were stained with a p65-specific antibody (SC-109; Santa Cruz Biotechnology, Inc.) and a Rhodamine RedX–conjugated goat anti–rabbit antibody (Jackson ImmunoResearch Laboratories) was added. Nuclei were stained with DAPI and coverslips were analyzed by fluorescence microscopy. Translocation of p65 to the nucleus was scored by enumerating the number of cells that had no nuclear staining (−), cells that displayed both cytoplasmic and nuclear staining (±), or cells that displayed bright nuclear staining and hardly any cytoplasmic staining (+).

DNA Manipulations and Sequence Analysis. Genomic DNA and total RNA were isolated from whole blood and the 5′ region of the *IKBA* gene and the promoter region were amplified by PCR using the primers described elsewhere (13, 15). Sequence analysis was performed using a Capillary Sequencer ABI 3700. For determination of wild-type versus mutated allele, PCR products generated using cDNA or genomic DNA as a template were digested with MspAI, which only digests the wild-type allele. In addition, the silent polymorphism in the father was determined by digestion with FokI, which only digests the polymorphic allele. Three different dilutions of the digested products were analyzed on a 2% agarose gel. The ratio of wild-type versus mutant allele in father and son were semiquantified by measuring the intensity of the undigested and digested band densitometrically, using a Gel Doc 2000 system (BioRad Laboratories) and Quantity One software (Bio-Rad Laboratories). To account for the size difference between the digested and undigested bands, the digestion efficiency of the two restriction enzymes, and possible exonuclease activity in the two restriction enzymes, ratios were corrected using an experimentally determined correction factor. For MspAI digests, which discriminate between wild-type and mutant alleles, this correction factor was obtained by setting the average intensity ratio found with genomic DNA of all cell types of the son, a true heterozygote, to 1, resulting in a correction factor of 3.7. The values for his mRNA and genomic DNA and mRNA of the father were corrected accordingly. A correction factor for FokI digests, which discriminate between the polymorphic and nonpolymorphic allele, was determined setting the average intensity ratio, obtained with DNA of the four other family members who are heterozygous for this polymorphism, to 1, resulting in a correction factor of 1.46. All other ratios were corrected using this factor.

Results

T and B Cell Function in the Patient. The patient presented with very high IgM levels, virtually no detectable IgG, and severe infection susceptibility. The other remarkable feature was a persistent lymphocytosis composed of CD4 and CD8 T cells at a normal ratio and virtually all expressing αβ TCRs. Further analysis revealed that >95% of both T cell subsets displayed a naive phenotype (i.e., $CD45RA^+$ [Table I], $CD27^+$, $CD28^+$, and $CCR7^+$ [not depicted]), indicating a maturation block. Flow cytometric and molecular analysis of the peripheral T cell compartment revealed a polyclonal Vβ repertoire (not depicted). Subnormal numbers of NK and B cells were present. In contrast, normal numbers of T and B lymphocytes and NK cells as well as normal serum Ig levels were present in both parents (Table I). Phenotypical analysis revealed relatively low

Downloaded from http://rupress.org/jem/article-pdf/200/5/559/1151690/jem2005559.pdf by guest on 29 May 2022

Table I. *Phenotype and Absolute Numbers of Blood Cells and Serum Ig Levels of the Patient, His Parents, and Controls*

	Patient (22 mo)	Father	Mother	Normal (15–24 mo)	Normal (adult)
Blood cells ($\times 10^9$ L)					
Leukocytes	18.1	5.3	10.2	6.8–10.0	4.3–10.0
Lymphocytes	14.3	1.6	1.7	2.7–11.9	1.0–2.8
Monocytes	1.4	0.9	0.9	unknown	0.2–1
T cells	13.6	1.1	1.3	1.4–8.0	0.7–2.1
$\gamma\delta$ T cells$^+$	<0.1	0.5	<0.1		
CD4$^+$ T cells	9.9	0.5	0.7	0.9–5.5	0.3–1.4
Naive (CD45RA)	9.5	0.1	0.3	1.1–3.6	0.2–0.9
Activated (CD45RO)	0.5	0.3	0.4	0.2–0.7	0.2–1
CD8$^+$ T cells	3.7	0.2	0.6	0.4–2.3	0.2–0.9
Naive (CD45RA)	3.7	<0.1	0.3	0.6–1.8	0.1–0.7
Activated (CD45RO)	0.1	0.1	0.3	<0.1–1	<0.1–0.5
B cells (CD19$^+$ CD20$^+$)	0.4	0.3	0.2	0.6–3.1	0.1–0.5
Serum Ig levels					
IgM (g/liter)	14.6	0.5	0.8	0.4–2.3	0.4–2.6
IgG (g/liter)	5.2[a]	14.6	9.9	3.5–11.4	6.6–18.4
IgA (g/liter)	<0.06	2.1	1.3	0.1–1.0	0.71–3.6
IgD (g/liter)	0.9	n.d.	n.d.	<0.2	

[a]After intravenous IgG supplementation, the IgG level was 0.5 g/liter before therapy.
n.d., not done.

numbers of naive CD4 and CD8 T cells in the father. In addition, an increased number of $\gamma\delta$ T lymphocytes were detected in the father. To determine T cell function, proliferative responses were measured after stimulation with various polyclonal activators and TT. Stimulation via TCR ligation by anti-CD3 mAbs or with PHA resulted in strongly impaired responses (Table II). These decreased responses could be partly overcome by additional costimulation with IL-2. Antigen-specific proliferation that was analyzed after three repetitive vaccinations with TT was completely absent. The proliferative response of the paternal T cells after stimulation with anti-CD3 was also impaired, albeit to a much lesser extent than in the child. The proliferative responses of the maternal T cells were unaffected. B cell proliferative responses were tested after stimulation with anti-CD40 and IL-4. Normal proliferative responses were measured in both the child and father (Table II).

IL-12p40 Production in Response to LPS. Monocyte function of the affected child and his parents was determined by culturing whole blood in the presence of increasing amounts of LPS. IL-12p40 production was completely absent in the child and, even at LPS concentrations up to 1,000 ng/ml, also hardly detectable in his father, whereas his mother and a control produced normal amounts of this cytokine (Fig. 1 A, black bars). This indicated that IL-12p40 production in response to LPS was not only impaired in the patient, but also in his father, who displays a completely different clinical phenotype.

To investigate whether IL-12p40 production could be induced when other TLR4 or TLR2 stimuli were used, whole blood was stimulated with *M. avium*, zymosan A, *S. aureus*, or PAM3CSK4. In contrast to the healthy control or the mother, none of the stimuli were able to induce significant amounts of IL-12p40 in father and son, indicating that a possible defect was downstream of the TLRs (Fig. 1 B).

To investigate whether IL-12p40 production could be up-regulated by IFN-γ, the combination of LPS and a high dose of IFN-γ (1,000 IU/ml) was used to stimulate whole

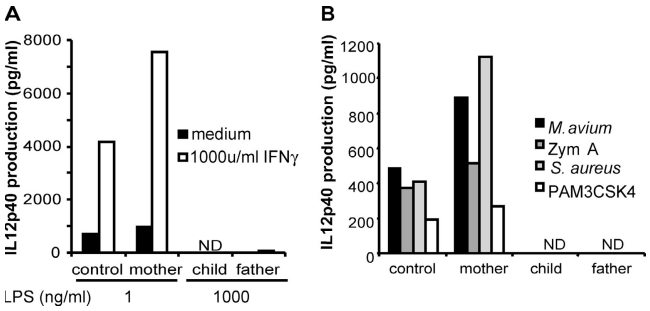

Figure 1. Production of IL-12p40 in whole blood of a healthy control, the mother, the father, and the child. (A) Whole blood was stimulated with LPS in the presence or absence of IFN-γ. (B) Whole blood was stimulated with 25 μg/ml *M. avium* sonicate, 100 μg/ml zymosan A, *S. aureus* (5×10^6 heat-killed bacteria/ml), and 200 ng/ml PAM3CSK4. Supernatants were collected after 18 h and IL-12p40 was measured by ELISA.

Downloaded from http://rupress.org/jem/article-pdf/200/5/559/1151690/jem2005559.pdf by guest on 29 May 2022

Table II. *T Cell Responses of the Patient and His Parents*

Cultured cells	Stimulus	Patient	Father	Mother
PBMCs	anti-CD3	0.3	59.5	350.1
	anti-CD3 + IL-2	15.5	155.0	433.5
	PHA	23.8	130.5	293.0
	PHA + IL-2	299.0	213.7	334.4
	none	<0.2	<0.2	<0.2
	TT preimmunization[a]	1	8.5	n.d.
	TT 6 wk after three immunizations[a]	1	n.d.	n.d.
$CD20^+$ B cells	anti-CD40 + IL-4	3.6	1.5	n.d.
	none	<0.05	<0.05	n.d.

Data are presented as cpm × 10^3 or [a]as stimulation index.
n.d., not done.

blood. In the child, IL-12p40 was still not detectable, but his father produced some IL-12p40, although the levels were very low (Fig. 1 A, white bars). This was confirmed at the level of mRNA production (not depicted).

Secretion of Other Cytokines in Whole Blood. Synthesis of IL-12p40 is dependent on NF-κB–activated transcription, suggesting that a possible defect was located in the NF-κB signal transduction pathway. Therefore, we also measured other cytokines that are induced upon NF-κB activation. Upon stimulation of whole blood with a high concentration of LPS, TNF-α and IL-1β production in the child were comparable to that of his father, mother, and the control (Fig. 2, A and C, black bars). On the other hand, IL-6 production was very low in the child but completely normal in his father (Fig. 2 B). These results indicate that not all of the NF-κB–dependent responses are impaired and that the functional defect in the child's monocytes was more severe than that in his father.

Another striking observation was that IFN-γ was not able to enhance TNF-α production in either father or son, whereas the mother and a healthy control up-regulated TNF-α production in the presence of IFN-γ (Fig. 2 A, white bars). This indicates that a possible defect in father and son results in impaired LPS responsiveness as well as impaired IFN-γ responsiveness of whole blood cells. It is important to note that IFN-γ concentrations up to 1,000 IU/ml were used in our assays, highlighting the true extent of IFN-γ unresponsiveness. IFN-γR expression was normal (not depicted).

IFN-γ Responsiveness Is Normal in Patient's PBMCs. To study the response to IFN-γ in more detail, monocytes were cultured in the presence of IFN-γ and the increase in expression of CD64 (FcγR1) was measured by FACS analysis. The CD64 promoter contains a STAT1 binding site and up-regulation of CD64 in response to IFN-γ stimulation is a well-accepted marker of IFN-γ responsiveness of cells. IFN-γ stimulation of control monocytes and those of the mother resulted in a dose-dependent increase in CD64 expression (Fig. 3). A dose-dependent increase was also seen in monocytes of father and son, although the maximal in-

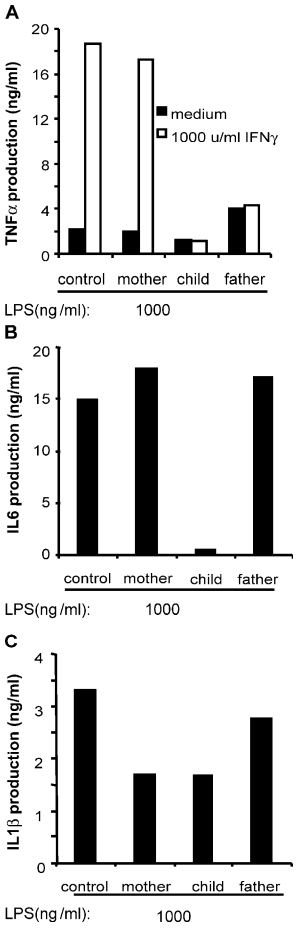

Figure 2. Production of other cytokines in whole blood. Whole blood was stimulated with LPS (A, B, and C) in the presence or absence of IFN-γ (A). Supernatants were collected after 18 h and TNF-α (A), IL-6 (B), and IL-1β (C) was measured by ELISA.

Downloaded from http://rupress.org/jem/article-pdf/200/5/559/1151690/jem2005559.pdf by guest on 29 May 2022

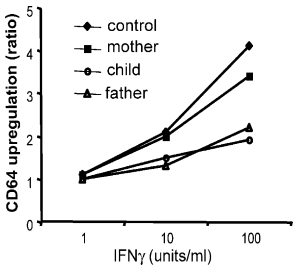

Figure 3. IFN-γ responsiveness of monocytes. PBMCs of a healthy control, the mother, the child, and the father were incubated for 18 h with increasing amounts of IFN-γ, and CD64 expression on CD14$^+$ monocytes was measured by FACS analysis. Data are expressed as the ratio of median fluorescence of cells cultured in the presence of IFN-γ over cells cultured in the absence of IFN-γ. The median fluorescence of unstimulated monocytes of the healthy control, the mother, the son, and the father was 66, 66, 145, and 90, respectively.

crease in CD64 expression reached was lower than for the healthy control and the mother (Fig. 3). Of note, the basal expression level of CD64 was higher in father and son, which may also partly have contributed to the reduced increase in expression in response to IFN-γ. The addition of 100 IU/ml IFN-γ to monocytes of father and son resulted in CD64 up-regulation comparable to that found in control monocytes stimulated with 10 U/ml IFN-γ. Thus, in contrast to what was found for TNF-α up-regulation in whole blood, significant IFN-γR signaling was detectable by measuring CD64 expression, such that IFN-γ responsiveness by this assay was only moderately affected.

Oxidative Burst. All data shown above indicate that TLR-induced signaling was impaired in the patient and his father. To investigate whether the defect was upstream of NF-κB activation or at the level of NF-κB itself, we measured the oxidative burst in formyl-methionyl-leucyl-phenylalanine–stimulated PMNs primed with either LPS or TNF-α. Only the first steps in the LPS and TNF-α signal transduction cascade are required to generate this response (16–18), and mutations at the level of the NF-κB complex itself are not expected to affect the oxidative burst. In healthy controls, the oxidative burst was enhanced 4.9- and 5.6-fold after priming with LPS and TNF-α, respectively. In the father, an enhanced oxidative burst was also observed upon LPS or TNF-α priming (2.2- and 2.8-fold, respectively), indicating that the defect was further downstream in the signal transduction cascade. PMNs of the child could not be tested.

Translocation of NF-κB to the Nucleus. Because all data pointed to a defect at the level of the NF-κB complex itself, we next studied p65 translocation to the nucleus in monocyte-derived macrophages stimulated with LPS. In control cells, ~90% of all monocytes displayed clear nuclear p65 staining after stimulation with LPS. In the child, p65 translocation was very inefficient (Fig. 4, A and B). First, fewer cells displayed nuclear staining. Second, the intensity of the nuclear staining was much lower in cells that did show translocation (scored as intermediate translocation). When macrophages of his father were tested, p65 translocation was also reduced, albeit to a lesser degree than in his son (Fig. 4 C). TNF-α stimulation was only used in

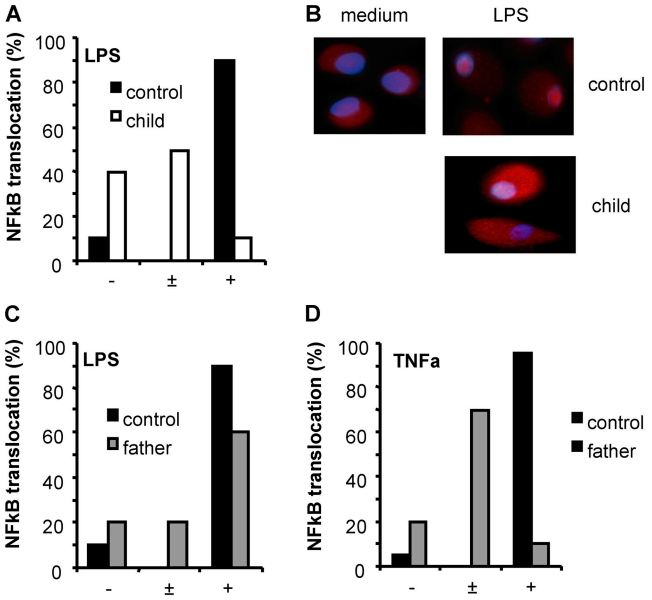

Figure 4. NF-κB translocation in monocyte-derived macrophages. Monocyte-derived macrophages were incubated with 1,000 ng/ml LPS (A, B, and C) or 200 U/ml TNF-α (D) for 45 min, and p65 translocation to the nucleus was analyzed (reference 14). Cells were stained with a p65-specific antibody, after which a Rhodamine RedX–conjugated goat anti–rabbit antibody was added. Nuclei were stained with DAPI and coverslips were analyzed by fluorescence microscopy (B). Translocation of p65 to the nucleus was scored by enumerating the number of cells that had no nuclear staining (−), cells that displayed intermediate nuclear staining (±), or cells that displayed bright nuclear staining (+).

the father and this stimulus also appeared to result in a lower level of p65 translocation (Fig. 4 D).

IκBα Mutation in Both Patients. Based on our clinical and functional data, and the phenotype of mice deleted in various NF-κB signaling components, genes encoding IKK1, IKK2, and IκB were the most likely candidates to investigate. During our investigations, Courtois et al. (13) published an *IKBA* mutation in a child with a clinical phenotype highly similar to that of our patient. Therefore, the sequence of *IKBA* was determined and a heterozygous G94T mutation was identified in both father and son resulting in a serine to isoleucine substitution at position 32. Serine 32 is one of the two serines that are phosphorylated by the IKK complex upon stimulation. After its phosphorylation, IκBα is ubiquitinated and targeted to the proteasome for breakdown, allowing NF-κB translocation to the nucleus. The heterozygosity of the mutation in both patients explains the residual activity found in our assays. The paternal grandmother, three siblings of the father, and the sibling and mother of the affected child did not display this mutation. The father, his three siblings, and the mother of the child were also heterozygous for a silent C/T polymorphism at position 80, whereas the child was homozygous for C at this position. The paternal grandmother of the child was homozygous for a C at position 80, indicating that it is likely that the mutation appeared de novo in her son (on his maternal allele) and was not

Downloaded from http://rupress.org/jem/article-pdf/200/5/559/1151690/jem2005559.pdf by guest on 29 May 2022

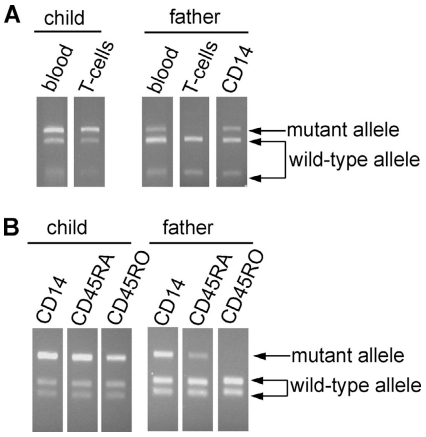

Figure 5. (A) Expression of wild-type versus mutated allele in whole blood, T cells, and monocytes. mRNA was isolated, cDNA was generated, and exon 1 of IκB was amplified by PCR. The PCR product was digested with MspA1, which only digests the wild-type allele. (B) Presence of wild-type versus mutated allele in monocytes, CD45RA, and CD45 RO cells of father and child. Genomic DNA was isolated from selected cell populations and exon 1 of IκB was amplified by PCR. The PCR product was digested with MspA1, which only digests the wild-type allele. Note that the size of the bands is different when DNA or RNA is used as a template for PCR.

passed on by the grandfather, who was not available for genetic testing.

Difference in Phenotype of Father and Son. Both patients showed the same mutation in IκBα. However, there is a striking difference between the disease severity of the father and his son. All functional data indicated that cell-mediated immune responses in the child, especially the T cell function, are more severely affected than in his father. One explanation for this difference could be that the residual NF-κB–mediated transcription in the father is higher than in his son. Several IκBα promoter polymorphisms that could account for this difference have been described and some of them appear to be associated with inflammation (15, 19). Because the mutation leads to the disappearance of a restriction site, it was possible to compare the expression of the healthy allele and the mutated allele. RNA was isolated from whole blood and used to generate cDNA. PCR was performed to amplify the 5′ part of the *IKBA* gene and the product was digested with MspAI. RNA isolated from blood samples taken with a 1-mo interval showed that in the child's whole blood, the wild-type allele and the mutant allele are expressed at an equal level. In the father, however, expression of the wild-type allele was higher than the mutant allele (Fig. 5 A and Table III). For comparison, the presence of the wild-type and mutant allele was also analyzed in genomic DNA. Both in the father and in the child the data obtained when genomic DNA was analyzed were similar to those found in the mRNA, indicating that in the father we are not dealing with a major difference in expression level of the two alleles, but with a mixed cell population.

Mosaicism in the Father. To ascertain whether we were indeed dealing with mosaicism, genomic DNA of various cell types of father and son were analyzed for the presence of the mutation. In the child, all cell types tested displayed the presence of equal amounts of wild-type and mutant allele (Table III). When whole blood, PMN, monocytes, buccalswab, and fibroblasts of the father were tested, it appeared that in all these cell types there was more wild-type allele than mutant allele present (Table III). Interestingly, the T and B cells of the father almost exclusively displayed

Table III. *Determination of the Ratio of Wild-type/Mutant Allele or Polymorphic/Nonpolymorphic Allele*

	Father			Son	
	Wild-type/mutant[b] (genomic DNA)	Wild-type/mutant (mRNA)	Polymorphic/nonpolymorphic[c] (genomic DNA)	Wild-type/mutant (genomic DNA)	Wild-type/mutant (mRNA)
Buccalswab (1)[a]	3.60 ± 0.94	ND	0.58 ± 0.41	ND	ND
Fibroblasts (1)	3.93 ± 0.42	4.12 ± 0.16	1.09 ± 0.05	0.83 ± 0.22	1.58 ± 0.08
Whole blood (3)	5.65 ± 0.94	7.66 ± 1.76	0.56 ± 0.13	0.98 ± 0.03	1.11 ± 0.05
PMN (2)	3.99 ± 0.2	6.72 ± 1.60	0.57 ± 0.24	1.03 ± 0.17	1.29 ± 0.01
Monocytes (2)	3.93 ± 0.1	9.03 ± 2.45	1.07 ± 0.05	1.17 ± 0.12	ND
T cells (3)	ND	41.1 ± 12.4	ND	ND	1.39 ± 0.18
CD45RA	9.89 ± 0.31	ND	1.16 ± 0.07	1.19 ± 0.10	ND
CD45RO	29.8 ± 0.92	ND±	1.20 ± 0.06	1.85 ± 0.26	ND
B cells	ND	24.00 ± 7.5	ND	ND	1.98 ± 0.08

[a]Data were obtained from (*n*) independent cell samples. Each sample was used at least twice for PCR, digestion, and quantification.
[b]Ratio of wild-type over mutant allele was determined using MspAI, which only digests the wild-type allele. Ratios were corrected using an experimentally determined correction factor, as described in Materials and Methods.
[c]Ratio of polymorphic over nonpolymorphic allele was determined using FokI, which only digests the polymorphic allele. Ratios were corrected using an experimentally determined correction factor, as described in Materials and Methods.

Downloaded from http://rupress.org/jem/article-pdf/200/5/559/1151690/jem2005559.pdf by guest on 29 May 2022

the wild-type allele. Because the father also had a silent polymorphism upstream of the mutation, the presence of this polymorphic allele was semiquantified. In the father, all cell types tested displayed equal amounts of the polymorphic allele and the nonpolymorphic allele, indicating that we are indeed dealing with mosaicism.

Selection of Wild-type Cells in the T and B Cell Compartment. All the data presented above point to mosaicism, hence the presence of a mixed cell population in the father. In T and B cells of the father, however, only the wild-type allele is present, suggesting that there is selection of wild-type cells in the T and B cell compartment. In murine models, it has been shown that memory T cell formation is dependent on NF-κB activation. Therefore, naive CD45RA and antigen-experienced CD45RO cells were isolated from the father, and the presence of the wild-type and mutant allele was determined. CD45RA cells clearly display the mutant allele, whereas CD45RO cells only display the wild-type allele (Fig. 5 B), indicating that in the father there is in vivo selection of wild-type cells in the T cell compartment.

Discussion

In this paper, we have identified a father and a son with a genetic mutation in *IκBα* replacing Ser 32, which is one of the two serines that are phosphorylated by the IKK complex upon stimulation. The signs and symptoms of the child are compatible with a mutation at this critical site, given the pivotal role of IκBα in signal transduction. He suffered from several severe infections in the first 6 mo of life and because of a hyper IgM-like syndrome, he received IgG supplementation and antibiotic prophylaxis. He has a persistent lymphocytosis of T cells that are mainly of a naive phenotype. The latter observation is consistent with the observations that NF-κB–mediated signal transduction is crucial for the development of mature T cells (20). During follow-up, typical clinical features of ectodermal dysplasia became increasingly evident. The same mutation was recently identified in a French patient with clinical symptoms almost identical to those of our patient (13). In contrast, the father of our patient, who has the same mutation but exhibits a complex mosaicism, does not display any of these symptoms. About 2 yr after discontinuation of steroid treatment for JIA, he experienced a recurrent invasive *S. typhimurium* infection. Finally, and after prolonged antibiotic treatment, he did not go through any more episodes of serious infection. This is the first report showing that the same IkBα mutation, which strongly impairs NF-κB–activated gene expression, can lead to two completely different clinical phenotypes.

Courtois et al. (13) have shown that a patient with the same mutation displayed severely impaired T cell function. We found identical features in our patient. In addition, we now show that monocyte function is also impaired. When responses to various PAMPs were evaluated, the most remarkable observation was that both father and son were unable to produce IL-12p40. However, normal levels of TNF-α and IL-1β were produced, and only the child displayed impaired IL-6 production. Because both father and son are heterozygous for the mutation, there is residual NF-κB activation as shown by our p65 translocation data. Due to the mosaicism in the father, the residual NF-κB activity in his mixed cell population is higher than that in his son. From our data, it is clear that not all NF-κB–mediated responses are affected to the same extent. Apparently, the dependence on NF-κB for various responses is graded where TNF-α and IL-1β production is unaffected when NF-κB activation is suboptimal, IL-6 production requires a higher level of activation, and IL-12p40 production requires optimal NF-κB activation. However, we have to take into account that TNF-α and IL-1β are released from preformed stores (a membrane-associated store for TNF-α and an intracellular store for IL-1β). Therefore, the levels of these cytokines measured in father and son might be largely independent of new synthesis. For TNF-α, we found that the level measured 4 h after the addition of LPS was similar to that found after 18 h (not depicted), which suggests that new synthesis may well be much slower in patients, although further studies are required to establish this.

The observation that not all promoters containing an NF-κB site are directly accessible (21) underlines our observation. Intriguingly, the IL-12p40 promoter only becomes accessible for the transcription machinery after histone modifications (22), which depend on activation of MAP kinases (22), indicating that stronger signals are required for IL-12p40 production. From previous studies in NEMO-deficient patients, it also became apparent that only a subset of NF-κB–activated responses was affected. In some patients, only CD40L-induced activation was severely hampered, whereas TLR4 activation by LPS remained largely intact (9), whereas in other NEMO patients LPS activation was hampered (23). More studies in patients with mutations in PAMP-induced signal transduction may contribute to further unravel this complex pathway.

Patients with defects in IL-12p40 or IL-12–induced signal transduction are susceptible to infections with intracellular pathogens like mycobacteria and *Salmonella*, and from a recent evaluation of patient data, the latter one appears to be especially prevalent in this patient group (24). Although we cannot rule out that the *Salmonella* infection in the father was related to long-term steroid treatment, it may instead be a result of his inability to produce IL-12p40. A possible role of the IκBα mutation and the consequent inability of monocytes to produce IL-12 in the pathogenesis and the disease course of JIA in the father are currently unclear.

The second striking feature found in our patients was the severely impaired IFN-γ response in whole blood of both father and son. This is consistent with the observations that MyD88 knockout mice are unable to mount a full-blown IFN-γ response (25). Because the genes for IL-12p40 and TNF-α are regulated by both NF-κB and STAT1, one could hypothesize that insufficient NF-κB activation would impair STAT1-mediated transactivation, a model

Downloaded from http://rupress.org/jem/article-pdf/200/5/559/1151690/jem2005559.pdf by guest on 29 May 2022

similar to the one proposed by Shi et al. (25). In addition, it has been shown that NF-κB activation leads to STAT1 phosphorylation on Ser727, which enhances its transcriptional activity (26, 27). Shi et al. (25) also showed that STAT1 phosphorylation on Tyr701 is normal in MyD88 knockout mice, indicating that impaired LPS responsiveness per se does not lead to reduced IFN-γ responsiveness. Consistent with this, our CD64 up-regulation assay, which is an indirect way of measuring STAT1-activated gene expression, i.e., Tyr701 phosphorylation, showed that this was only somewhat impaired in our patient. This could be attributable to reduced Ser727 phosphorylation, although it is important to point out that basal expression levels of CD64 in father and son were enhanced as compared with those found in controls, which may also have accounted for the lower degree of up-regulation observed. Apparently transactivation of TNF-α production is impaired in the patients, whereas direct activation of the IFN-γ–responsive CD64 gene remains largely intact. This may still preclude full activation of the macrophages' antimicrobial mechanisms and contribute to the infection susceptibility of the patients. In addition, it may hamper Th1 cell development.

The discrepancy in phenotype between father and son remains the most intriguing finding in this dominant negative genetic disease. Genetic analysis of the paternal grandmother revealed that the mutation arose de novo in the father. This fits well with the observed mosaicism in the father and suggests that the mutation arose early in embryonic development, leading to a mixture of wild-type and mutant cells. Because the T and B cell compartment of the father is almost exclusively composed of wild-type cells, one has to hypothesize that during T and B cell development or activation, these wild-type cells have a selective advantage over mutant cells. The observation that memory T cell activation in mice is highly dependent on NF-κB activation underscores this hypothesis. When naive, CD45RA and activated CD45RO cells were analyzed, it appeared that only naive cells display the mutant allele, indicating that there is in vivo selection of wild-type cells in the T cell compartment of the father. This is consistent with studies in murine models where NF-κB activation was shown to be crucial for development of mature T cells (20).

We conclude that the same IκBα mutation can not only be found in patients with typical ectodermal dysplasia and severe immunodeficiency affecting innate and adaptive immunity, but also in individuals that do not display any of the typical features expected to be associated with this defect. The attenuated clinical disease of the father is a result of a complex mosaicism and selection of wild-type–expressing cells in the T and B cell compartment. Because the amount of residual NF-κB activation in father and son appears to determine the severity of disease, further studies should focus on the evaluation of the NF-κB activation pathway in larger groups of patients that do not display the typical features that are thought to be associated with defects in this pathway. Although TLR-mediated NF-κB activation is thought to be crucial to combat infections, there appears to be a high level of redundancy, even in this signal transduction cascade.

This work was supported by the Netherlands Organization for Scientific Research and the Royal Netherlands Academy for Arts and Sciences.

The authors have no conflicting financial interests.

Submitted: 19 April 2004
Accepted: 13 July 2004

References

1. O'Brien, A.D., D.L. Rosenstreich, I. Scher, G.H. Campbell, R.P. MacDermott, and S.B. Formal. 1980. Genetic control of susceptibility to *Salmonella typhimurium* in mice: role of the LPS gene. *J. Immunol.* 124:20–24.
2. Feng, C.G., C.A. Scanga, C.M. Collazo-Custodio, A.W. Cheever, S. Hieny, P. Caspar, and A. Sher. 2003. Mice lacking myeloid differentiation factor 88 display profound defects in host resistance and immune responses to *Mycobacterium avium* infection not exhibited by toll-like receptor 2 (TLR2)- and TLR4-deficient animals. *J. Immunol.* 171:4758–4764.
3. Mun, H.S., F. Aosai, K. Norose, M. Chen, L.X. Piao, O. Takeuchi, S. Akira, H. Ishikura, and A. Yano. 2003. TLR2 as an essential molecule for protective immunity against *Toxoplasma gondii* infection. *Int. Immunol.* 15:1081–1087.
4. Takeuchi, O., K. Hoshino, and S. Akira. 2000. Cutting edge: TLR2-deficient and MyD88-deficient mice are highly susceptible to *Staphylococcus aureus* infection. *J. Immunol.* 165: 5392–5396.
5. Seki, E., H. Tsutsui, N.M. Tsuji, N. Hayashi, K. Adachi, H. Nakano, S. Futatsugi-Yumikura, O. Takeuchi, K. Hoshino, S. Akira, et al. 2002. Critical roles of myeloid differentiation factor 88-dependent proinflammatory cytokine release in early phase clearance of *Listeria monocytogenes* in mice. *J. Immunol.* 169:3863–3868.
6. Edelson, B.T., and E.R. Unanue. 2002. MyD88-dependent but Toll-like receptor 2-independent innate immunity to *Listeria*: no role for either in macrophage listericidal activity. *J. Immunol.* 169:3869–3875.
7. Medzhitov, R. 2001. Toll-like receptors and innate immunity. *Nat. Rev. Immunol.* 1:135–145.
8. Li, Q., and I.M. Verma. 2002. NF-kappaB regulation in the immune system. *Nat. Rev. Immunol.* 2:725–734.
9. Jain, A., C.A. Ma, S. Liu, M. Brown, J. Cohen, and W. Strober. 2001. Specific missense mutations in NEMO result in hyper-IgM syndrome with hypohydrotic ectodermal dysplasia. *Nat. Immunol.* 2:223–228.
10. Picard, C., A. Puel, M. Bonnet, C.L. Ku, J. Bustamante, K. Yang, C. Soudais, S. Dupuis, J. Feinberg, C. Fieschi, et al. 2003. Pyogenic bacterial infections in humans with IRAK-4 deficiency. *Science.* 299:2076–2079.
11. Medvedev, A.E., A. Lentschat, D.B. Kuhns, J.C. Blanco, C. Salkowski, S. Zhang, M. Arditi, J.I. Gallin, and S.N. Vogel. 2003. Distinct mutations in IRAK-4 confer hyporesponsiveness to lipopolysaccharide and interleukin-1 in a patient with recurrent bacterial infections. *J. Exp. Med.* 198:521–531.
12. Gerondakis, S., M. Grossmann, Y. Nakamura, T. Pohl, and R. Grumont. 1999. Genetic approaches in mice to understand Rel/NF-kappaB and IkappaB function: transgenics and knockouts. *Oncogene.* 18:6888–6895.

Downloaded from http://rupress.org/jem/article-pdf/200/5/559/1151690/jem2005559.pdf by guest on 29 May 2022

13. Courtois, G., A. Smahi, J. Reichenbach, R. Doffinger, C. Cancrini, M. Bonnet, A. Puel, C. Chable-Bessia, S. Yamaoka, J. Feinberg, et al. 2003. A hypermorphic IkappaBalpha mutation is associated with autosomal dominant anhidrotic ectodermal dysplasia and T cell immunodeficiency. *J. Clin. Invest.* 112:1108–1115.
14. Straus, D.S., G. Pascual, M. Li, J.S. Welch, M. Ricote, C.H. Hsiang, L.L. Sengchanthalangsy, G. Ghosh, and C.K. Glass. 2000. 15-deoxy-delta 12,14-prostaglandin J2 inhibits multiple steps in the NF-kappa B signaling pathway. *Proc. Natl. Acad. Sci. USA.* 97:4844–4849.
15. Mozzato-Chamay, N., E.L. Corbett, R.L. Bailey, D.C. Mabey, J. Raynes, and D.J. Conway. 2001. Polymorphisms in the IkappaB-alpha promoter region and risk of diseases involving inflammation and fibrosis. *Genes Immun.* 2:153–155.
16. Yan, S.R., W. Al Hertani, D. Byers, and R. Bortolussi. 2002. Lipopolysaccharide-binding protein- and CD14-dependent activation of mitogen-activated protein kinase p38 by lipopolysaccharide in human neutrophils is associated with priming of respiratory burst. *Infect. Immun.* 70:4068–4074.
17. McLeish, K.R., C. Knall, R.A. Ward, P. Gerwins, P.Y. Coxon, J.B. Klein, and G.L. Johnson. 1998. Activation of mitogen-activated protein kinase cascades during priming of human neutrophils by TNF-alpha and GM-CSF. *J. Leukoc. Biol.* 64:537–545.
18. Zu, Y.L., J. Qi, A. Gilchrist, G.A. Fernandez, D. Vazquez-Abad, D.L. Kreutzer, C.K. Huang, and R.I. Sha'afi. 1998. p38 mitogen-activated protein kinase activation is required for human neutrophil function triggered by TNF-alpha or FMLP stimulation. *J. Immunol.* 160:1982–1989.
19. Abdallah, A., H. Sato, J.C. Grutters, S. Veeraraghavan, P.A. Lympany, H.J. Ruven, J.M. van den Bosch, A.U. Wells, R.M. du Bois, and K.I. Welsh. 2003. Inhibitor kappa B-alpha (IkappaB-alpha) promoter polymorphisms in UK and Dutch sarcoidosis. *Genes Immun.* 4:450–454.
20. Schmidt-Supprian, M., G. Courtois, J. Tian, A.J. Coyle, A. Israel, K. Rajewsky, and M. Pasparakis. 2003. Mature T cells depend on signaling through the IKK complex. *Immunity.* 19:377–389.
21. Saccani, S., S. Pantano, and G. Natoli. 2001. Two waves of nuclear factor κB recruitment to target promoters. *J. Exp. Med.* 193:1351–1359.
22. Saccani, S., S. Pantano, and G. Natoli. 2002. p38-Dependent marking of inflammatory genes for increased NF-kappa B recruitment. *Nat. Immunol.* 3:69–75.
23. Zu, Y.L., J. Qi, A. Gilchrist, G.A. Fernandez, D. Vazquez-Abad, D.L. Kreutzer, C.K. Huang, and R.I. Sha'afi. 1998. p38 mitogen-activated protein kinase activation is required for human neutrophil function triggered by TNF-alpha or FMLP stimulation. *J. Immunol.* 160:1982–1989.
24. Ottenhoff, T.H., F.A. Verreck, E.G. Lichtenauer-Kaligis, M.A. Hoeve, O. Sanal, and J.T. van Dissel. 2002. Genetics, cytokines and human infectious disease: lessons from weakly pathogenic mycobacteria and salmonellae. *Nat. Genet.* 32:97–105.
25. Shi, S., C. Nathan, D. Schnappinger, J. Drenkow, M. Fuortes, E. Block, A. Ding, T.R. Gingeras, G. Schoolnik, S. Akira, et al. 2003. MyD88 primes macrophages for full-scale activation by interferon-γ yet mediates few responses to *Mycobacterium tuberculosis*. *J. Exp. Med.* 198:987–997.
26. Kovarik, P., D. Stoiber, P.A. Eyers, R. Menghini, A. Neininger, M. Gaestel, P. Cohen, and T. Decker. 1999. Stress-induced phosphorylation of STAT1 at Ser727 requires p38 mitogen-activated protein kinase whereas IFN-gamma uses a different signaling pathway. *Proc. Natl. Acad. Sci. USA.* 96: 13956–13961.
27. Kovarik, P., D. Stoiber, M. Novy, and T. Decker. 1998. Stat1 combines signals derived from IFN-gamma and LPS receptors during macrophage activation. *EMBO J.* 17:3660–3668.

Downloaded from http://rupress.org/jem/article-pdf/200/5/559/1151690/jem2005559.pdf by guest on 29 May 2022